Pakistan Veterinary Journal

ISSN: 0253-8318 (PRINT), 2074-7764 (ONLINE)
DOI: 10.29261/pakvetj/2026.163

RESEARCH ARTICLE

Essential Oil of *Cymbopogon nardus* Disrupts Osmoregulation and Cuticle Integrity in Parasitic Nematode

Chintianna Widhi Atthahirah[1], Penny Humaidah Hamid[1,2,*], Herjuno Ari Nugroho[3], Syahputra Wibowo[4] and Nur Balqis Maulydia[4]

[1]Faculty of Animal Science, Universitas Sebelas Maret, Indonesia, [2]Tropical Onehealth and Ecohealth Institute, Indonesia, [3]Research Center for Applied Microbiology, National Research and Innovation Agency, Indonesia, [4]Eijkman Research Center for Molecular Biology, National Research and Innovation Agency, Indonesia
*Corresponding author: pennyhumaidahhamid@staff.uns.ac.id

ARTICLE HISTORY (26-311)

Received: March 27, 2026
Revised: May 26, 2026
Accepted: June 02, 2026
Published online: July 15, 2026

Key words:
Anthelmintic
Ascaridia galli
Essential oil
Ethnopharmacology
Infectious disease

ABSTRACT

Ascaridia (*A.*) *galli* is a gastrointestinal nematode that causes significant economic losses in poultry production worldwide. The emergence of anthelmintic resistance and concerns regarding chemical residues have stimulated interest in plant-based alternatives. *Cymbopogon nardus* essential oil (CNEO) has demonstrated various biological activities; however, its anthelmintic potential against *A. galli* and the possible underlying mechanisms remain poorly characterised. Herein, CNEO was tested *in vitro* against adult *A. galli* worms. Mortality data were analysed by a generalised linear mixed model (GLMM) with binomial error and logit link, with treatment, exposure time and their interaction as fixed effects and replicate as a random factor. CNEO produced concentration- and time-dependent mortality, reaching 100% by 80min at 10% and by 160min at 1% ($P<0.001$ versus the pooled NaCl control; Cohen's $h\approx2.92$ at both concentrations). Scanning electron microscopy (SEM) confirmed cuticular roughening, lip distortion and abnormal annulation patterns. Histology of treated worms showed cuticular deformation, fragmentation of cortical and fibrous layers, and disruption of ovarian structures with egg deformation. Predictive molecular docking of the three principal monoterpenoids, citronellal, citronellol and geraniol, against aquaporin (AQP), glutamate-gated chloride channel (GluCl), nicotinic acetylcholine receptor (nAChR) and Na^+/K^+-ATPase revealed favourable binding energies (ΔG in kcal/mol): citronellal gave -6.2 (AQP), -5.1 (GluCl), -4.5 (nAChR) and -4.8 (Na^+/K^+-ATPase); citronellol gave -6.4, -5.0, -4.6 and -4.7, respectively; geraniol gave -6.6, -5.1, -4.8 and -5.0, respectively. Residue-level interaction analyses showed that citronellol formed the most diverse contacts at nAChR (including Pi-alkyl, Pi-sigma and hydrogen bonds), whereas geraniol consistently exhibited the strongest hydrophobic networks at AQP and Na^+/K^+-ATPase. Importantly, the predicted binding energies of the three monoterpenoids at nAChR (-4.5 to -4.8kcal/mol) are comparable to those of the reference nAChR-specific drugs levamisole (-5.1) and pyrantel pamoate (-5.4). Furthermore, CNEO exhibits a complementary multi-target profile that could potentiate or synergise with existing anthelmintics, positioning it may act as a complementary adjuvant candidate. Further, functional validation by bio-guided fractionation and target-specific assays is recommended.

To Cite This Article: Atthahirah CW, Hamid PH, Nugroho HA, Wibowo S and Maulydia NB, 2026. Essential oil of *Cymbopogon nardus* disrupts osmoregulation and cuticle integrity in parasitic nematode. Pak Vet J, 46(7): 1695-1707. http://dx.doi.org/10.29261/pakvetj/2026.163

INTRODUCTION

Chicken meat is one of the leading sources of animal protein and among the most widely consumed meats globally (Nassar, 2025). However, the intensification of poultry production systems has been accompanied by increased challenges related to disease management, particularly parasitic infections that compromise animal productivity (Salem *et al.*, 2025). One important parasite is *Ascaridia* (*A.*) *galli*, a nematode of the family Ascaridiidae

that infects the small intestine of chickens and other galliform birds (Höglund *et al.*, 2023). This parasitic nematode has a direct life cycle, with embryonated eggs ingested by birds from contaminated environments, followed by larval development within the intestinal mucosa before returning to the lumen as adult worms (Bennett *et al.*, 2023; Höglund *et al.*, 2023). *A. galli* infection is associated with reduced weight gain, decreased egg production, intestinal obstruction, and increased susceptibility to secondary infections, resulting in substantial economic losses (Shohana *et al.*, 2023). The control of gastrointestinal nematodes in poultry has traditionally relied on synthetic anthelmintic drugs, including benzimidazoles, imidazothiazoles and macrocyclic lactones. However, the repeated and often indiscriminate use of these chemotherapeutic agents has led to the emergence of anthelmintic resistance (Sajid *et al.*, 2022; Kapo *et al.*, 2025).

In response to these challenges, plant-derived products have attracted increasing attention as natural antiparasitic agents. Essential oils, in particular, are valued for their complex chemical composition and the potential for multiple mechanisms of action (Matté *et al.*, 2023; Ristanti *et al.*, 2024; Hernando *et al.*, 2025; Zoroaster *et al.*, 2025). For instance, *trans*-cinnamaldehyde from cinnamon (*Cinnamomum* sp.) essential oil acts on multiple Cys-loop receptor targets, including levamisole-sensitive nicotinic acetylcholine receptors, GABA-activated chloride channels and glutamate-activated chloride channels, and has been shown to act synergistically with classical anthelmintics (Hernando *et al.*, 2025). Star anise (*Illicium verum*) essential oil produced dose-dependent reductions in faecal egg counts and reduced egg hatchability and worm motility in *A. galli* (Rasheed and Aljohani, 2024), while clove (*Syzygium aromaticum*) oil at 2-6% caused parasite mortality within 11h by disrupting glucose uptake, glycogen content and oxygen consumption (Nagaich, 2022). Bioactive compounds such as flavonoids, tannins, saponins and triterpenoids have been implicated in these anthelmintic effects (Zirintunda *et al.*, 2021; Roy *et al.*, 2022). *Cymbopogon* (*C.*) *nardus* is a perennial aromatic grass of the Poaceae family, widely cultivated in tropical regions of Asia, Africa and the Americas (Nakahara *et al.*, 2013). The essential oil extracted from *C. nardus*, commonly known as citronella oil, has been used traditionally as an insect repellent, antifungal agent and fragrance component (Trindade *et al.*, 2022; Uopasai *et al.*, 2024). Citronellal, citronellol, and geraniol are repeatedly reported as its dominant monoterpene constituents (Nakahara *et al*., 2013; Wei and Wee, 2013; Saputra *et al*., 2020; Kaur *et al*., 2021; Sukandar *et al*., 2022). However, the anthelmintic activity of *C. nardus* essential oil (CNEO) against nematodes, particularly *A. galli*, and its underlying mechanisms have not been comprehensively investigated.

The present study was designed to investigate the anthelmintic activity of CNEO against adult *A. galli* using *in vitro* assays. To complement these biological observations and generate mechanistic hypotheses, predictive molecular docking was performed using the three major constituents of CNEO, citronellal, citronellol, and geraniol, against four pharmacologically relevant nematode targets: aquaporin (AQP), glutamate-gated chloride channels (GluCl), nicotinic acetylcholine receptors (nAChR), and Na^+/K^+-ATPase. The predicted binding interactions were also compared with those of conventional anthelmintic compounds.

MATERIALS AND METHODS

Parasite collection: Adult *A. galli* worms were retrieved from the small-intestinal lumen of free-range chickens (*Gallus gallus domesticus*) routinely slaughtered for human consumption at Ngebong Market, Boyolali Regency, Indonesia. Worms were placed immediately in 50mL sterile conical tubes containing pre-warmed (37°C) phosphate-buffered saline (PBS, pH 7.4), transported to the laboratory within 2h, and transferred to fresh 0.9% NaCl (warmed to 37°C) for adaptation. Only macroscopically intact, actively motile worms were used. All experimental treatments were initiated within 3h of post-collection (Ristanti *et al.*, 2023).

CNEO source: Steam-distilled CNEO was obtained from a local supplier (Rumah Atsiri, Central Java, Indonesia) and stored in amber glass vials until use.

***In vitro* anthelmintic assay:** The *in vitro* assay was performed using the adult-worm immersion approach adapted from Vijaya and Yadav (2016) and Lalthanpuii and Lalchhandama (2020). CNEO was serially diluted in 0.9% NaCl to give five working concentrations: 10%, 1%, 0.1%, 0.01% and 0.001% (v/v); these are coded P2K1-P2K5, where P denotes "*Perlakuan*" (treatment) and K denotes "*Konsentrasi*" (concentration). The control (P1) was 0.9% NaCl warmed to 37°C. Each working solution (5mL) was poured into a sterile watch glass; ten adult worms (n=10 per replicate) were transferred into each watch glass with non-surgical forceps so that the worms were fully immersed. Mortality was assessed at 10, 20, 40, 80 and 160min after exposure. A worm was scored as dead when it remained motionless for 30sec of continuous observation under a stereomicroscope and showed no response to gentle mechanical stimulation with a blunt probe at three different body regions; provisionally non-motile worms were transferred to fresh 0.9% NaCl at 37°C and re-examined after 5min, and only those that failed to regain motility were recorded as dead (Vijaya and Yadav, 2016). Each treatment was run in four independent biological replicates (n=4), giving 40 worms per treatment per time point.

The 160min observation time was selected on the basis of three considerations: (i) *A. galli* adult worms maintained in 0.9% NaCl at 37°C in our preliminary trials remained viable (>95%) for at least 4h, beyond which background mortality became non-negligible and would confound treatment effects; (ii) the 10-, 20-, 40-, 80-, 160min logarithmic schedule resolves the rapid onset of action expected for a membrane-active monoterpene mixture (Nagaich, 2022; Hernando *et al.*, 2025); and (iii) all treatment groups had reached either 100% or a clear plateau in mortality by 160min, so prolonging the assay would not have changed the rank order of treatments. We did not include a positive (synthetic-anthelmintic) reference group *in vitro* because the present study was designed as a first characterisation of CNEO's nematicidal effect against adult *A. galli*. While ivermectin, levamisole and pyrantel pamoate are slow-acting on adult *A. galli* under static

immersion (Lalthanpuii and Lalchhandama, 2020). A direct *in vitro* comparison with reference anthelmintics is identified as a priority for follow-up work, and these three drugs were nevertheless included as *in silico* docking controls (see below).

Histological examination: Histology was processed at the Anatomical Pathology Laboratory, Faculty of Medicine, Universitas Gadjah Mada, Indonesia. Adult *A. galli* specimens exposed to the highest CNEO concentration (10%) for the longest observation time (160min) were selected for tissue analysis to evaluate internal structural damage; control worms received 0.9% NaCl for the same duration. Three worms per group (n=3) were processed in parallel and examined by an observer blinded to treatment allocation. Worms were fixed in 10% neutral-buffered formalin for 24h, dehydrated through a graded ethanol series, cleared in xylene and embedded in paraffin. Cross-sections of 5µm were cut on a rotary microtome, mounted, and stained with haematoxylin and eosin (H&E). At least five non-overlapping fields per section and three sections per worm were examined under a light microscope (Olympus, Japan) at 100X magnification.

Scanning electron microscopy: Adult *A. galli* worms (three per group, n=3) from the 10% CNEO and NaCl control groups were processed for SEM at the Genomic Laboratory, BRIN, Indonesia. Worms were rinsed three times in 0.1M cacodylate buffer (pH 7.4), fixed in 2.5% glutaraldehyde in the same buffer for 24h at 4°C, post-fixed in 1% osmium tetroxide for 2h, and dehydrated through a graded ethanol series (30, 50, 70, 80, 90% and 3×100%, 15min each). Specimens were critical-point-dried in CO_2, mounted on aluminium stubs with carbon tape, sputter-coated with a thin gold layer (≈10nm) and examined with a JSM-IT200 SEM (JEOL, Japan) at 10kV at magnifications between 100X and 40,000X. Anterior, mid-body and posterior regions of each worm were photographed.

Molecular docking protocol: Predictive molecular docking was carried out for citronellal, citronellol and geraniol against four pharmacologically relevant nematode targets: aquaporin (AQP, UniProt Q19949), glutamate-gated chloride channel α (GluCl, PDB 3RHW), nicotinic acetylcholine receptor non-α subunit (nAChR, UniProt Q17328) and Na^+/K^+-ATPase β-1 subunit (UniProt Q93235). All four sequences/structures originate from *Caenorhabditis elegans*. Use of *C. elegans* as a structural surrogate for *A. galli* was justified by their shared placement in class Chromadorea, order Rhabditia, and by the conserved residues lining each binding cavity within these protein families across nematode clades; orthologue alignments and conservation of binding-site residues were inspected before docking.

Protein and ligand preparations: Structures of the four target proteins were retrieved from the Protein Data Bank (PDB) for GluCl (3RHW) and from UniProt homology models for the remaining three receptors. Crystallographic waters, co-crystallised ligands and other non-essential heteroatoms were removed; biologically relevant cofactors were retained (Berman *et al*., 2002). Ligand structures (citronellol PubChem CID 8842; geraniol CID 637566; citronellal CID 7794) were obtained in SDF format, converted to PDB, and geometrically optimised while preserving rotatable bonds. For citronellol and geraniol, the following additional pre-processing steps were applied: (i) the dominant protonation state at pH 7.4 was assigned using Open Babel (default pH-dependent algorithm); (ii) energy minimisation was performed with the MMFF94 force field (steepest descent, 500 steps) to relieve local steric clashes; (iii) the exhaustiveness parameter for the subsequent docking search was set to 8 (the CB-Dock2 default, balancing speed and sampling depth).

Cavity detection and docking grid definition: Cavity prediction was performed with the P2Rank machine-learning method (Krivak and Hoksza, 2018) and further refined with CurPocket as implemented in CB-Dock2 (Liu *et al*., 2022).

Docking validation via redocking of co-crystallised ligand (3RHW): To validate the docking protocol, the co-crystallised ligand of the *C. elegans* GluCl channel (PDB 3RHW), ivermectin, was extracted and re-docked into the same receptor using the identical grid parameters derived from its own cavity. The root-mean-square deviation (RMSD) between the re-docked ivermectin pose and the experimentally determined X-ray pose was 0.87Å (below the 2.0Å threshold for successful pose reproduction), confirming the reliability of the docking procedure.

Docking calculations and pose selection: All docking calculations were performed with the CB-Dock2 server (version 2022), an automated blind-docking platform that integrates cavity detection with the AutoDock Vina scoring function (Liu *et al*., 2022; Eberhardt *et al*., 2021). All ligands, citronellal, citronellol, geraniol and the three anthelmintic drugs (ivermectin CID 6321424, levamisole CID 26879, pyrantel pamoate CID 4953), were docked under identical parameters (exhaustiveness = 8, otherwise server defaults) to ensure direct comparability of binding energies and interaction patterns. For each receptor, ligand pair, the optimal pose was selected on the basis of (i) the most negative binding free energy (kcal/mol), (ii) localisation within a biologically relevant cavity and (iii) overlap with known active-site residues. Hydrogen bonds, hydrophobic contacts, π-π stacking and electrostatic interactions were analysed using BIOVIA Discovery Studio Visualizer 21.1.0 (Wibowo *et al*., 2024; Situmorang *et al*., 2025). Three reference anthelmintics, ivermectin, levamisole and pyrantel pamoate, were docked under identical parameters as positive *in silico* controls.

Statistical analysis: Mortality data (number of dead worms/total worms per replicate) are bounded proportional counts and were therefore analysed with a generalised linear mixed model (GLMM) with binomial error and logit link, fitted in R 4.4.1 with the *lme4* package. Treatment, exposure time and their interaction were entered as fixed effects, and replicate was a random effect. Type-III Wald χ^2 tests were used for fixed effects; pairwise post-hoc contrasts were obtained with *emmeans* using Tukey adjustment for multiple comparisons. Because the five P1 (NaCl) sub-groups were pre-specified as identical replicate

controls (and verified statistically: $\chi^2(4)=1.13$, P=0.889), they were pooled for presentation. Effect sizes versus the pooled NaCl control at each time point were quantified as Cohen's *h* for proportions (conventions: *h*≈0.2 small, 0.5 medium, 0.8 large, >1.2 very large). Two-sided 95% confidence intervals (Wilson score, truncated at the biological boundaries [0, 100]) are reported alongside means±SD in Table 1. Significance was set at P<0.05. Sample size (n=4replicates × 10 worms=40 worms per treatment per time point) was determined *a priori* for a two-proportion comparison detecting a difference of 50% versus 0% with α=0.05 and power 1-β=0.95 (G*Power 3.1; n≈8 per group); the chosen design therefore provides ample power for the observed effect sizes.

RESULTS

In vitro anthelmintic activity of CNEO: CNEO produced concentration- and time-dependent mortality of adult *A. galli* (Table 1, Fig. 1). The treatment×time interaction was highly significant ($\chi^2(24)=312.4$, P<0.001). At 10% (P2K1), mortality reached 50.0±25.8% within 10min and 100% by 80min. At 1% (P2K2), mortality rose progressively to 100% by 160min. Lower concentrations were substantially less active: 0.1% (P2K3) reached 37.5±45.0% only at 160min, while 0.01% (P2K4) and 0.001% (P2K5) produced only modest, non-significant mortality at 160min (35.0±10.0% and 15.0±19.2%, respectively). The five sub-groups of the NaCl control did not differ from each other ($\chi^2(4)=1.13$, P=0.889) and remained at 0% throughout, justifying their pooling for analysis and display. Effect sizes versus the pooled NaCl control at 160min were very large for P2K1 and P2K2 (Cohen's *h*=2.92 each) and large for P2K3, P2K4 and P2K5 (*h*=1.32, 1.27 and 0.80, respectively). Tukey-adjusted pairwise contrasts are summarised in Table 1.

Histological alterations: In control worms (NaCl, 160min) the cuticle showed an intact cortical (exocuticle) and fibrous (endocuticle) layer with normal structural organisation, and reproductive structures showed typical ovoid eggs with smooth, thick eggshells and compact internal contents (Fig. 2A-C). Worms exposed to 10% CNEO for 160min showed marked cuticular deformation and fragmentation, with a serrated cortical layer and disruption of the fibrous layer with partial separation and fusion of structural fibres. Reproductive structures were also altered: ovaries appeared irregular with dissociation and deformation of egg cells (Fig. 2D-F).

Scanning electron microscopy: Control worms showed normal external morphology, with three well-defined dentigerous lips around the oral opening (two subventral, one dorsal) and a smooth mid-body cuticle with regularly spaced annulations (Fig. 3A-C). Worms exposed to 10% CNEO showed clear morphological alterations (Fig. 3D-F): the anterior region was contracted and folded with more prominent annulations; cuticular surfaces were rough and wrinkled with deflation and collapse of the lips; and the mid-body cuticle showed marked roughness, abnormal longitudinal and transverse folds, and irregularly arranged annulations.

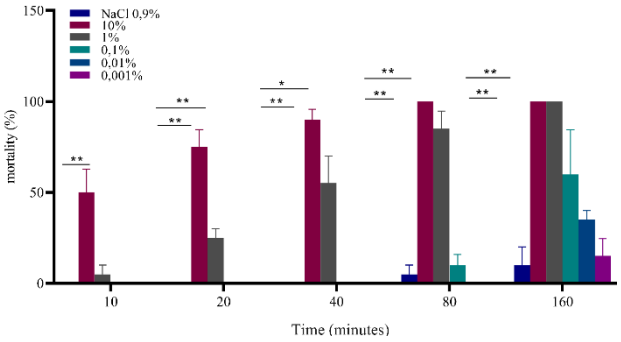

Fig. 1: Mortality of adult *A. galli* exposed to CNEO at five concentrations over a 160min observation window. CNEO produced concentration- and time-dependent mortality (treatment × time interaction: $\chi^2(24)=312.4$, P<0.001). Significant differences from the pooled NaCl control were observed at 10% and 1% from 10 and 20min onwards respectively (P<0.05); the lower concentrations (0.1%, 0.01%, 0.001%) and the NaCl control were not significantly different at most time points. Values are mean±SD of n=4 replicates (10 worms each).

Table 1: Mean percentage mortality (±SD) of adult *A. galli* exposed to CNEO and 0.9% NaCl control over a 160min observation period (n=4 replicates per condition; 10 worms per replicate). Different uppercase letters within the same row denote significant differences among observation times for that treatment (Tukey-adjusted, P<0.05). Asterisks denote a significant difference from the pooled NaCl control at the same time point (P<0.05). Numbers in italic parentheses are 95% confidence intervals

Treatment	Conc. (%)	10 min	20 min	40 min	80 min	160 min
P1 (NaCl, pooled)	-	0.0±0.0 A (0.0–0.0)	0.0±0.0 A (0.0–0.0)	0.0±0.0 A (0.0–0.0)	0.0±0.0 A (0.0–0.0)	0.0±0.0 A (0.0–0.0)
P2K1 (CNEO)	10	50.0±25.8 B* (8.9-91.1)	75.0±19.2 BC* (44.5-100.0)	90.0±11.6 CD* (71.6-100.0)	100.0±0.0 D* (100.0)	100.0±0.0 D* (100.0)
P2K2 (CNEO)	1	5.0±10.0 A (0.0-20.9)	25.0±10.0 B* (9.1-40.9)	55.0±30.0 C* (7.3-100.0)	85.0±19.2 D* (54.5-100.0)	100.0±0.0 D* (100.0)
P2K3 (CNEO)	0.1	0.0±0.0 A (0.0–0.0)	0.0±0.0 A (0.0–0.0)	0.0±0.0 A (0.0–0.0)	10.0±11.6 AB (0.0-28.4)	37.5±45.0 B* (0.0-100.0)
P2K4 (CNEO)	0.01	0.0±0.0 A (0.0–0.0)	0.0±0.0 A (0.0–0.0)	0.0±0.0 A (0.0–0.0)	0.0±0.0 A (0.0–0.0)	35.0±10.0 B* (19.1-50.9)
P2K5 (CNEO)	0.001	0.0±0.0 A (0.0–0.0)	0.0±0.0 A (0.0–0.0)	0.0±0.0 A (0.0–0.0)	0.0±0.0 A (0.0–0.0)	15.0±19.2 AB (0.0-45.5)

Notes. Values are mean±SD; numbers in italic parentheses on the second line of each cell are 95% confidence intervals (lower–upper bound), computed from the t-distribution on *n*=4 replicate means. Confidence intervals are truncated at the biological boundaries [0, 100]. Where SD=0, no interval is shown. Statistical analysis. Mortality counts (dead worms / total worms per replicate) were modelled using a generalised linear mixed model (GLMM) with binomial error and logit link, with treatment, exposure time, and their interaction as fixed effects, and replicate as a random effect, fitted with the *lme4* package in R 4.4.1. Type-III Wald χ^2 tests were used for fixed effects; pairwise post-hoc contrasts were obtained with *emmeans* using Tukey adjustment for multiple comparisons. Effect of treatment × time was significant ($\chi^2(24) = 312.4$, P<0.001). The five P1 (NaCl) sub-groups did not differ ($\chi^2(4) = 1.13$, P=0.889) and were pooled for presentation. Superscripts. Different uppercase letters within the same row denote significant differences among observation times for that treatment (Tukey-adjusted, P<0.05). Asterisks (*) denote a significant difference from the pooled NaCl control at the same time point (Tukey-adjusted, P<0.05). Effect sizes (Cohen's *h*) versus control at 160min: P2K1=2.92, P2K2=2.92, P2K3=1.32, P2K4=1.27, P2K5=0.80. Conventions: *h*≈0.2 small, 0.5 medium, 0.8 large, >1.2 very large. Abbreviations: P1=NaCl 0.9% (control); P2=CNEO; K1–K5=serial dilutions (10%, 1%, 0.1%, 0.01%, 0.001% v/v in NaCl 0.9%).

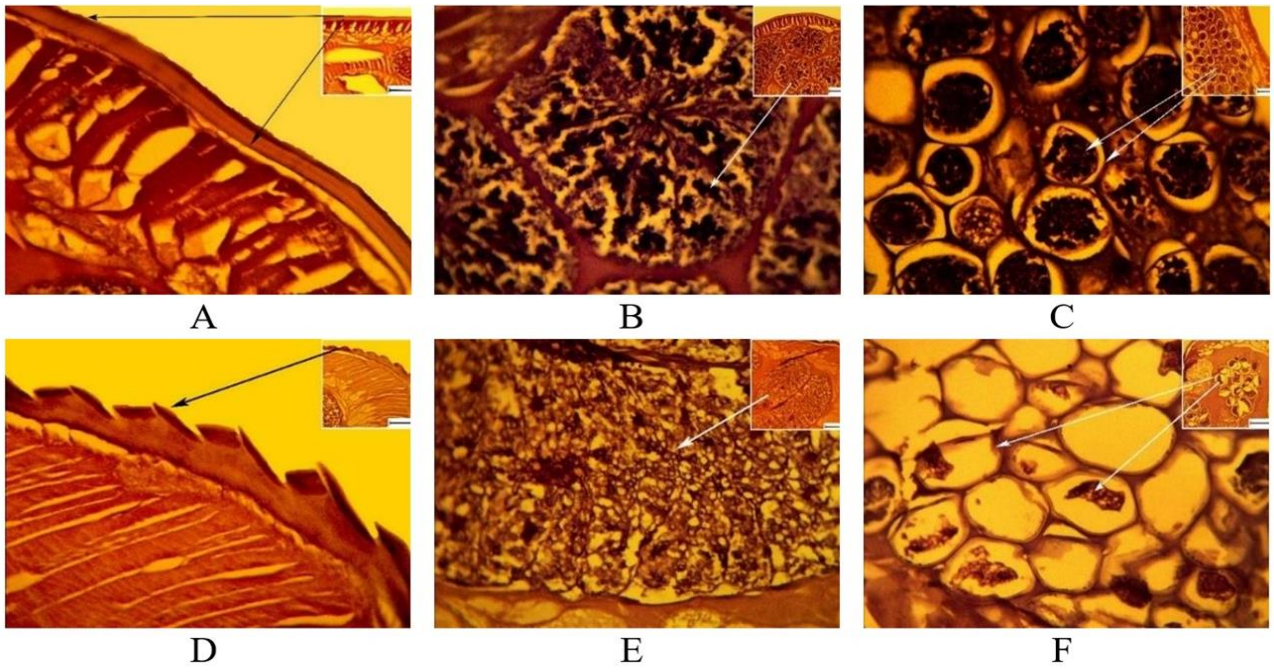

Fig. 2: Histological cross-sections (H&E) of adult *A. galli*. (A-C) Control worms (0.9% NaCl, 160min) showing intact cuticle layers with normal exocuticle and endocuticle and well-preserved ovarian and egg morphology. (D-F) Worms exposed to 10% CNEO for 160min showing cuticular deformation, fragmentation and serrated appearance of the cortical layer (exocuticle), disruption and fusion of the fibrous layers (endocuticle), irregular ovarian structure and deformation/dissociation of egg cells. Scale bars=10µm.

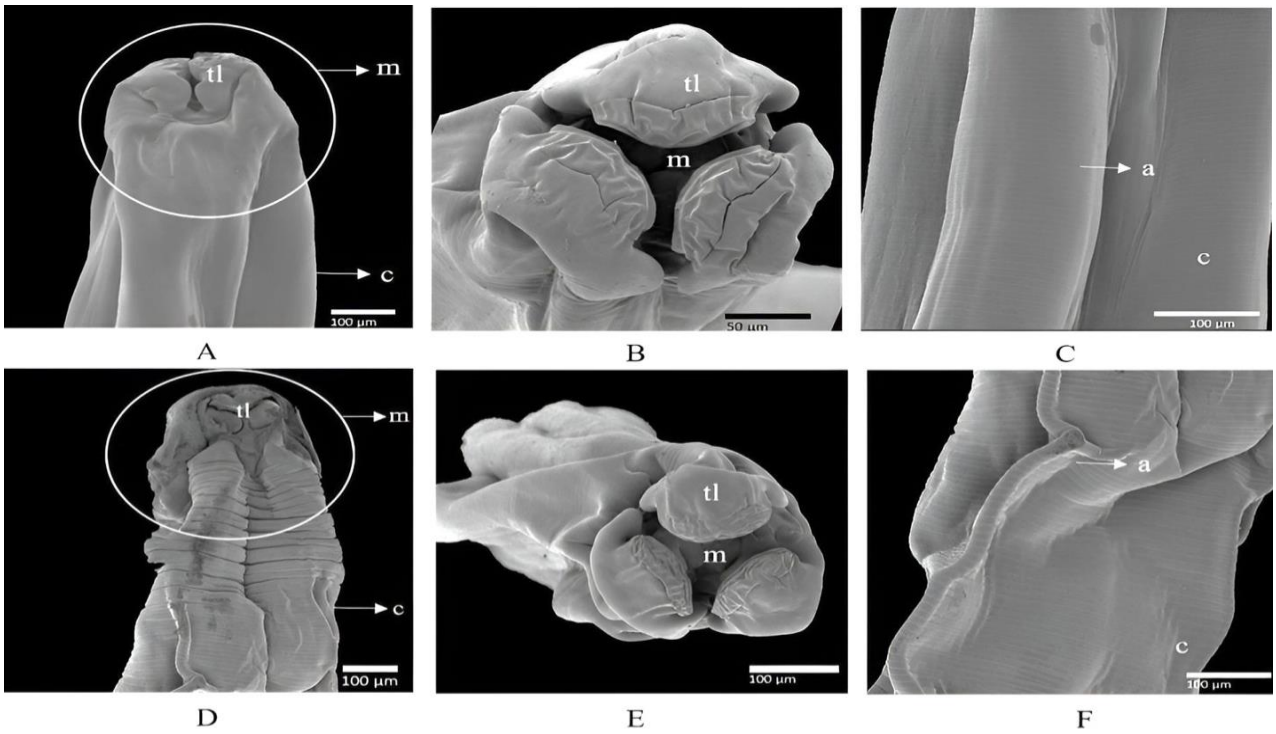

Fig. 3: Scanning electron microscopy of adult *A. galli* in control (A-C) and after treatment with CNEO (D-F). (A) Anterior region of control worms immersed in 0.9% NaCl, showing normal lateral lips (tl) surrounding the mouth (m). (B) Frontal view of the control mouth showing three well-defined dentigerous lips. (C) Mid-body cuticular surface (c) of control worms, smooth with faint annulations (a). (D) Anterior region of treated worms showing contraction and body folding, more prominent annulations, roughened and irregularly wrinkled cuticle and deflated lips. (E) Mouth region of treated worms showing distortion of the three dentigerous lips. (F) Mid-body cuticular surface of treated worms showing marked roughness, clearly visible annulations and abnormal irregular folding.

Molecular docking: Predicted binding pockets for the four nematode targets (AQP, GluCl, nAChR, Na^+/K^+-ATPase) and the residues lining each cavity are summarised in Table 2. Citronellal, citronellol, and geraniol were selected as representative major constituents of citronella oil based on previous reports (Nakahara *et al*., 2013; Wei and Wee, 2013; Saputra *et al*., 2020; Kaur *et al*., 2021; Sukandar *et al*., 2022). The predicted docking binding free energies of the tested molecules and the three reference anthelmintics, ivermectin, levamisole, and pyrantel pamoate, are summarised in Table 3. Docking interaction maps grouped by receptor are shown in Fig. 4 (AQP), 5 (GluCl), 6 (nAChR), and 7 (Na^+/K^+-ATPase).

Table 2: P2Rank-predicted active sites for the four nematode receptors used in molecular docking.

Protein (database ID)	Predicted active-site residues
UniProt Q17328 - nicotinic acetylcholine receptor (nAChR), non-α subunit	Ile71(A), Val73(A), Tyr168(A), Asn211(A), Phe212(A), Arg243(A), Tyr247(A), Tyr248(A), Lys298(A), Leu299(A) 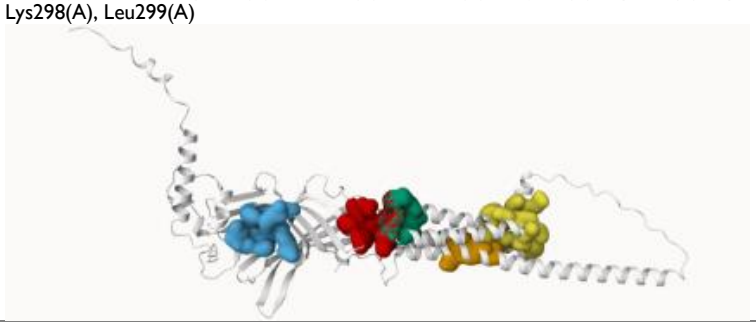
UniProt Q19949 - aquaporin (AQP)	Val53(A), Phe56(A), His57(A), Trp66(A), Val69(A), Trp73(A), Ile147(A), Leu148(A), Gly149(A), Gly152(A), Gly155(A), Ala158(A), Ser159(A), Tyr160(A), Ser162(A), Gly216(A), Met217(A), Asn218(A), Ile219(A), Gly220(A), Arg227(A) 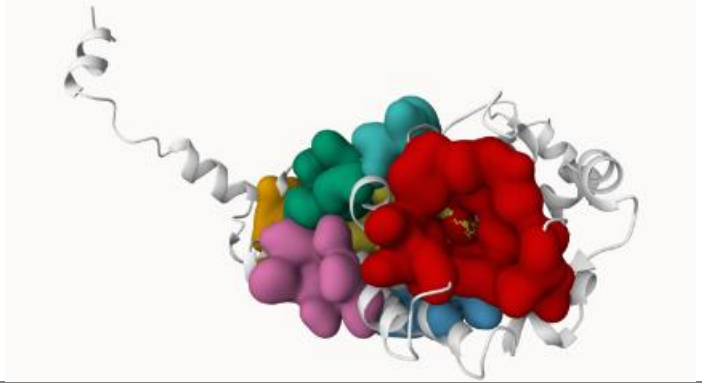
UniProt Q93235 - Na^+/K^+-ATPase β-1 subunit	Leu134(A), Asp138(A), Leu169(A), Phe172(A), Asp173(A), Ser177(A), Glu178(A) 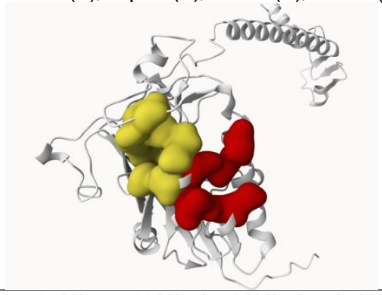
PDB 3RHW - GluCl	Phe91(C), Pro93(C), Asn94(C), Ser129(C), Pro131(C), Ser145(C), Asp147(C), Ala149(C), Ser150(C), Tyr151(C), Cys191(C), Ser193(C), Thr195(C), Thr197(C), Tyr200(C), Cys202(C), Arg204(C), Leu35(D), Arg37(D), Thr38(D), Thr54(D), Arg56(D), Leu109(D), Ser121(D), Lys171(D), Val172(D), Gly173(D) 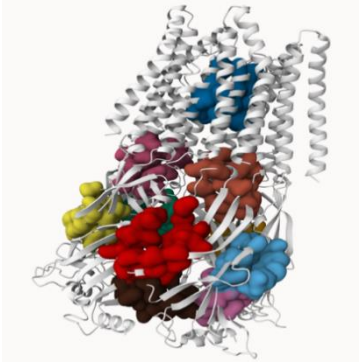

Note. Active-site residues were predicted with P2Rank (Krivak and Hoksza, 2018) and refined with CB-Dock2 cavity detection (Liu *et al*., 2022). All four sequences/structures originate from *C. elegans* and are used as orthologue surrogates for *A. galli* (see Materials and methods).

Citronellal showed affinities across all targets, with ΔG ranging from -6.2 (AQP) to -4.5 (nAChR) kcal/mol. At AQP (-6.2kcal/mol; Fig. 4A), the citronellal complex was stabilised by conventional and carbon-hydrogen bonds together with alkyl, Pi-sigma and Pi-alkyl hydrophobic contacts, although the presence of an unfavourable acceptor-acceptor term suggested that the aldehyde group may adopt a suboptimal orientation, potentially limiting binding in an aqueous environment. At GluCl (-5.1kcal/mol; Fig. 5A), a single conventional hydrogen bond and a Pi-sigma interaction (involving PHE A:386, PRO A:390, LEU A:271, ARG A:277) were predicted, with no alkyl or Pi-alkyl contacts, a much simpler profile than that of ivermectin at the same target. At nAChR, citronellal showed

the weakest predicted binding energy among the tested ligands (-4.5kcal/mol; Fig. 6A). However, the 2D interaction output did not show a clearly defined residue-level interaction pattern for this complex, whereas levamisole and pyrantel pamoate displayed more distinct receptor contacts. At Na^+/K^+-ATPase (-4.8kcal/mol; Fig. 7A), conventional and carbon-hydrogen bonds plus alkyl interactions involved VAL A:171, PRO A:246, PHE A:167, LYS A:220 and TYR A:254, and the absence of Pi-contacts together with the modest energy imply that citronellal may only weakly associate with the ion pump.

Table 3: Molecular docking binding free energies of ligands and reference anthelmintic drugs.

Ligand	AQP	GluCl	nAChR	Na^+/K^+-ATPase
Citronellal	-6.2	-5.1	-4.5	-4.8
Citronellol	-6.4	-5.0	-4.6	-4.7
Geraniol	-6.6	-5.1	-4.8	-5.0
Ivermectin	-9.3	-9.4	-	-8.4
Levamisole	-	-	-5.1	-
Pyrantel pamoate	-	-	-5.4	-

Note: Predicted molecular-docking binding free energies (kcal/mol) of citronellal, citronellol, geraniol and three reference anthelmintics against four nematode targets. "-" indicates that the ligand was not docked at that target (selective control).

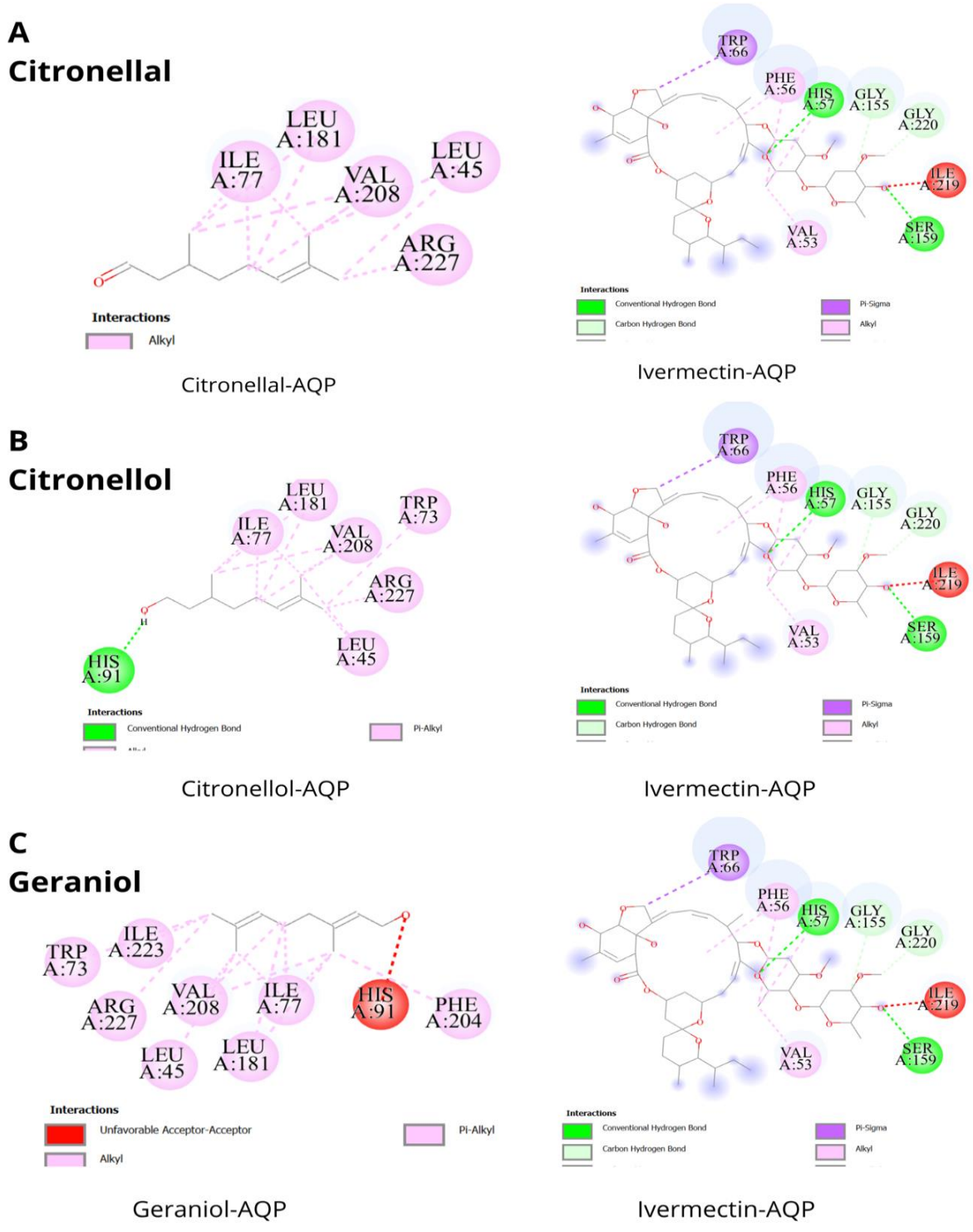

Fig. 4: Comparative AQP docking interaction profiles. Predicted residue-level interaction maps of citronellal, citronellol, and geraniol docked into the aquaporin binding pocket (AQP; UniProt ID: Q19949), compared with ivermectin as the reference anthelmintic. Panels show: (A) citronellal, (B) citronellol, and (C) geraniol. Interaction types are colour-coded according to the legend in each sub-panel.

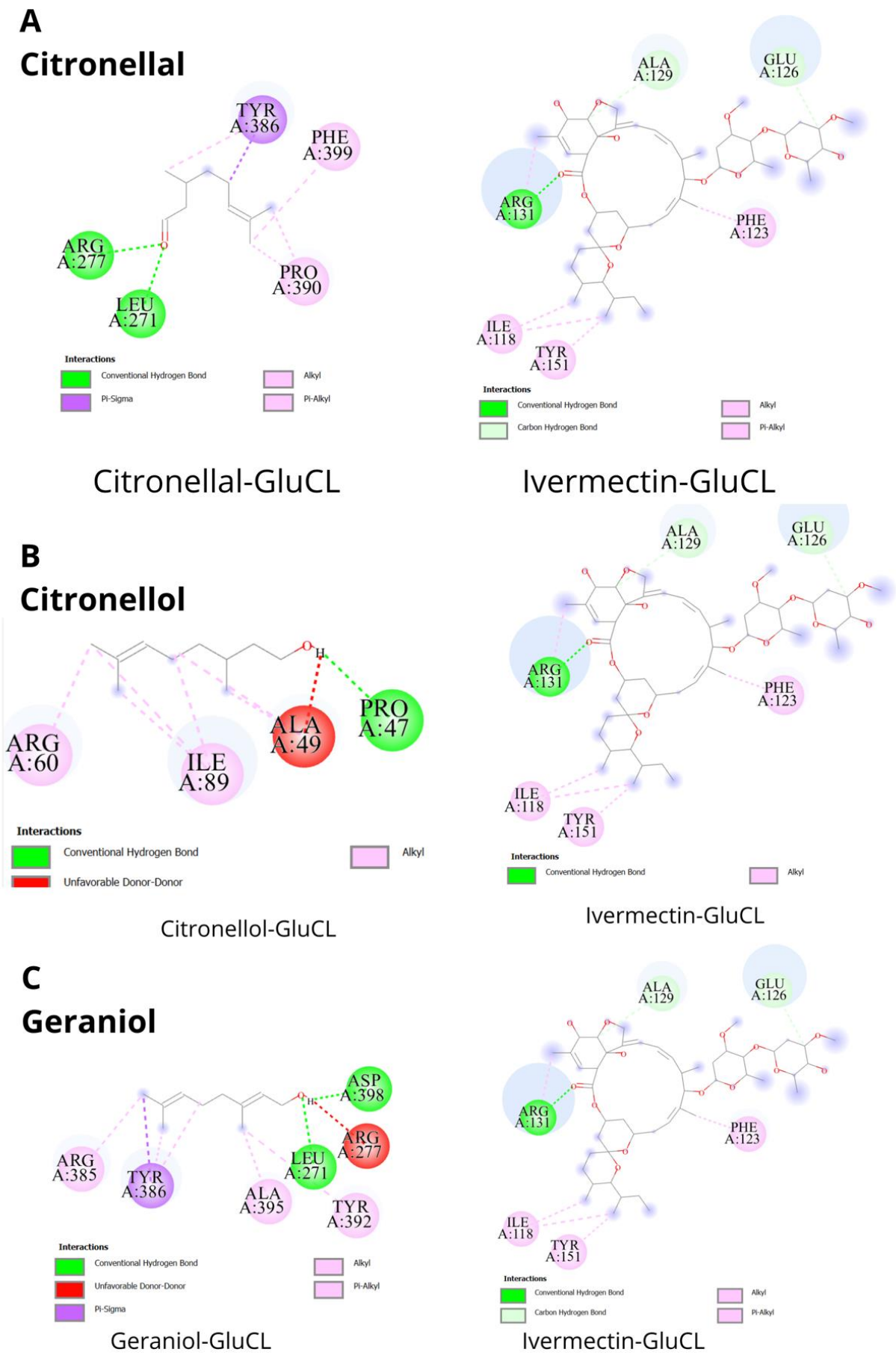

Fig. 5: Predicted ligand–GluCl binding interactions. Two-dimensional interaction maps showing the binding profiles of the principal CNEO monoterpenoids within the glutamate-gated chloride channel pocket (GluCl), alongside ivermectin as the reference compound. Panels represent the docking contacts formed by citronellal (A), citronellol (B), and geraniol (C), including hydrogen bonds, hydrophobic interactions, Pi-associated contacts, and unfavourable interactions.

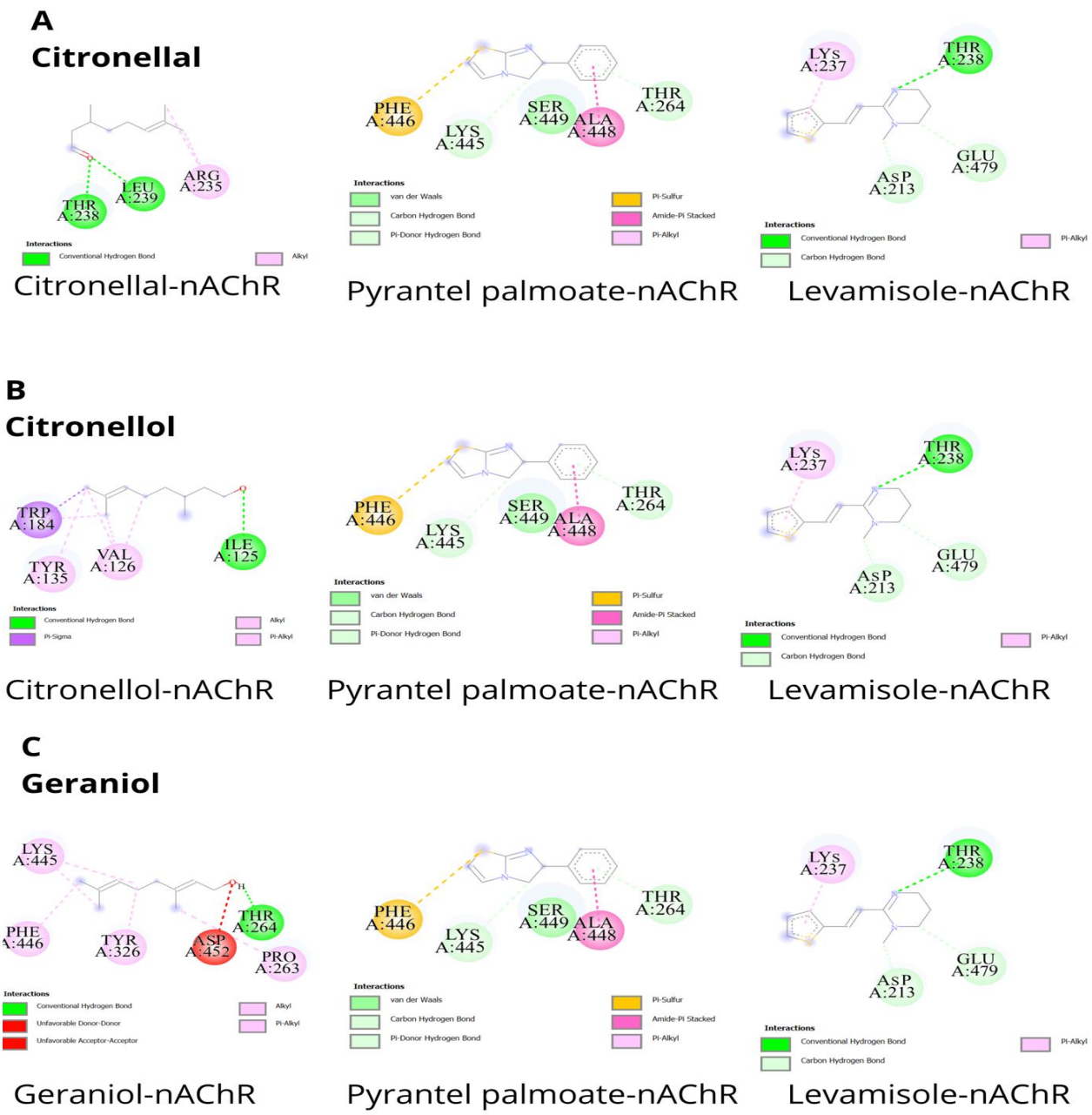

Fig. 6: Comparative docking patterns at the nAChR binding site. Residue-level interaction maps of citronellal (A), citronellol (B), and geraniol (C) docked into the nicotinic acetylcholine receptor non-α subunit (nAChR; UniProt ID: Q17328). Levamisole and pyrantel pamoate were included as reference anthelmintics. Panels show compound-specific interaction profiles and comparative contact patterns within the predicted receptor pocket.

Citronellol produced slightly more favourable binding energies than citronellal, particularly at AQP (-6.4) and nAChR (-4.6). At AQP (Fig. 4B), a conventional hydrogen bond with HIS A:91 was accompanied by Pi-alkyl (involving A:181, TRP A:73, VAL A:208, ARG A:227, LEU A:45, and again HIS A:91), Pi-sigma, alkyl, and carbon-hydrogen bond contacts, plus an unfavourable acceptor-acceptor interaction, and the involvement of a hydrogen bond via the hydroxyl group may explain the slightly stronger affinity relative to citronellal. At GluCl (-5.0kcal/mol; Fig. 5B), a conventional hydrogen bond and alkyl interactions were predicted with ILE E:280, A:219, GLN A:218, MET E:284 and A:222, with no Pi-type interactions, whereas ivermectin engages this target through a broader hydrophobic network consistent with its much higher potency. At nAChR (Fig. 6B), citronellol displayed the most diverse interaction network among the monoterpenoids at this receptor: conventional hydrogen bonds (VAL A:126, TYR A:135), carbon-hydrogen bonds, a Pi-donor hydrogen bond, and hydrophobic contacts including Pi-alkyl (LYS A:446, PHE A:446, LYS A:445), Pi-sigma (THR A:237, ALA A:448), Pi-sulfur and amide-Pi stacking. Despite this richness, the binding energy (-4.6kcal/mol) remained slightly below those of levamisole (-5.1) and pyrantel pamoate (-5.4), suggesting that citronellol may occupy the orthosteric site but, lacking a quaternary ammonium group, is unlikely to act as a strong agonist. At Na^+/K^+-ATPase (-4.7kcal/mol; Fig. 7B), a conventional hydrogen bond and a Pi-sigma interaction involved VAL A:171, TYR A:254, PHE A:167 and PRO A:246, with no alkyl contacts reported, and the binding mode is distinct from that of ivermectin (which uses multiple alkyl and Pi-alkyl interactions) and is predicted to be weak.

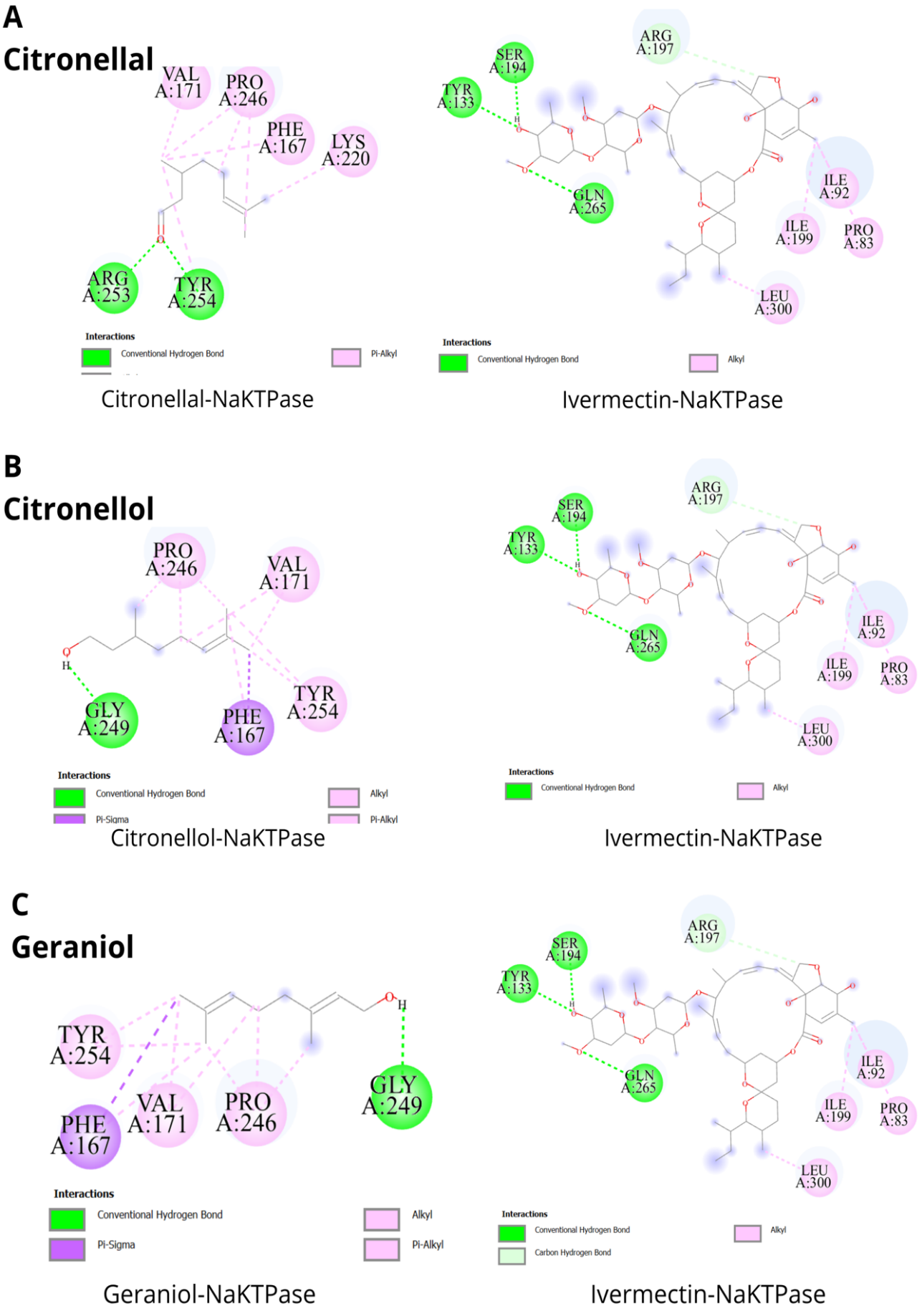

Fig. 7: Na^+/K^+-ATPase docking interaction map. Predicted binding interactions of the three major CNEO monoterpenoids with the Na^+/K^+-ATPase β-1 subunit binding pocket (UniProt ID: Q93235), using ivermectin as the reference anthelmintic. Panels compare citronellal (A), citronellol (B), and geraniol (C) against ivermectin, with interaction types indicated by the colour legend.

Geraniol consistently yielded the strongest binding energies among the three monoterpenoids for every target, with ΔG values of -6.6 (AQP), -5.1 (GluCl), -4.8 (nAChR) and -5.0 (Na^+/K^+-ATPase), aligning with prior evidence that geraniol possesses anthelmintic activity against gastrointestinal nematodes. At AQP (Fig. 4C), geraniol was stabilised by conventional and carbon-hydrogen bonds along with alkyl hydrophobic contacts involving a wide set of residues (TRP A:73, ILE A:220, VAL A:207, ARG A:227, LEU A:45, ILE A:77, HIS A:91, PHE A:204), and an unfavourable acceptor-acceptor interaction was also noted; compared with ivermectin, geraniol's extra double bond may permit more extended hydrophobic contacts, though the overall affinity remains far lower. At GluCl (-5.1kcal/mol; Fig. 5C), a conventional hydrogen bond and a Pi-sigma interaction were predicted (no specific residues extractable), and an unfavourable donor-donor contact was noted, with the binding energy matching that of citronellal but the interaction appearing limited. At nAChR (Fig. 6C), the complex was characterised by a conventional hydrogen bond together with unfavourable donor-donor and acceptor-acceptor interactions, and crucially, no hydrophobic interactions (alkyl, Pi-alkyl, Pi-sigma) were reported; the presence of two unfavourable terms suggests that geraniol may be forced into a strained orientation within the binding pocket, which could offset its slightly better binding energy (-4.8) compared to citronellol (-4.6). At Na^+/K^+-ATPase (-5.0kcal/mol; Fig. 7C), geraniol exhibited the most favourable predicted interaction among the three monoterpenoids, with conventional hydrogen bonding, Pi-sigma, alkyl and Pi-alkyl contacts involving a broad set of residues: TYR A:254, VAL A:171, PRO A:246, PHE A:167, GLY A:249, ARG A:197, SER A:194, ILE A:92, ILE A:199, PRO A:83 and LEU A:300; this comparatively rich hydrophobic network may explain why geraniol's ΔG reaches -5.0, approaching the range of weak inhibitors.

DISCUSSION

CNEO showed concentration- and time-dependent anthelmintic activity against adult *A. galli*, with very large effect sizes at 10% and 1% (Cohen's $h \approx 2.92$) and complete mortality reached by 80 and 160min, respectively. These findings extend the growing literature on plant-derived essential oils as natural anthelmintic candidates (Carvalho *et al.* Nagaich, 2022; 2023; Frota *et al.*, 2023; Matté *et al.*, 2023; Rasheed and Aljohani, 2024; Hernando *et al.*, 2025). Both the CNEO concentrations and the time course needed for full mortality are within the range reported for clove and star-anise oils against the same host-parasite system (Nagaich, 2022; Rasheed and Aljohani, 2024).

A. galli is a cylindrical nematode whose body is covered by a multilayered, collagen-rich cuticle composed of cortical (exocuticle), matrix (mesocuticle) and fibrous (endocuticle) layers, with regular transverse annulations that confer flexibility and resistance to host digestive enzymes (Decraemer *et al.*, 2003; Basyoni and Rizk, 2016). The anterior bears three dentigerous lips and amphidial chemoreceptors that mediate feeding and host sensing. In our SEM observations, worms exposed to 10% CNEO showed widespread cuticular roughening, lip distortion and abnormal annulation, while histology revealed fragmentation of the cortical and fibrous layers and disruption of ovarian structures with egg deformation. Together, these observations indicate that CNEO compromises the protective and selective-permeability functions of the cuticle and reaches internal organs. Comparable cuticular damage has been reported in *A. galli* treated with pyrantel pamoate (Lalthanpuii and Lalchhandama, 2020) and in other nematodes exposed to plant-derived phenolic and terpenoid agents (Balqis *et al.*, 2017; Martinez-Ortiz-de-Montellano *et al.*, 2019; Ali *et al.*, 2021).

Chemical surveys of citronella oils from different geographic origins have identified citronellal, citronellol, and geraniol as principal monoterpene constituents (Nakahara *et al*., 2013; Wei and Wee, 2013; Kaur *et al*., 2021; Saputra *et al*., 2020; Sukandar *et al*., 2022). Although direct anthelmintic activity of citronellol against *A. galli* has not, to our knowledge, been described, the structurally related monoterpene alcohol geraniol has demonstrated activity against gastrointestinal nematodes (Frota *et al.*, 2023), supporting our decision to take both compounds forward into predictive docking to predict binding to the four selected nematode targets.

Across all four targets, the three monoterpenoids formed mainly conventional hydrogen bonds and hydrophobic contacts, including alkyl, Pi-alkyl, and Pi-sigma interactions, but lacked the extensive high-affinity networks observed with ivermectin. Geraniol showed the strongest predicted affinities, particularly at AQP and Na^+/K^+-ATPase, suggesting that it may contribute most to the multi-target binding profile of CNEO. However, unfavourable interactions in some complexes, such as geraniol-nAChR and citronellal-AQP, indicate possible suboptimal docking poses that may be altered by induced-fit effects or water-mediated contacts in a dynamic biological system. Similarly, the absence of clearly visualised residue-level contacts for the citronellal-nAChR complex, despite its predicted binding energy, suggests marginal receptor engagement or a docking pose that did not meet the interaction-distance thresholds used for 2D annotation. If functionally confirmed, the predicted interactions could have the following physiological consequences: binding to AQP might disrupt osmoregulation, contributing to cuticular swelling and the morphological damage observed by SEM; weak GluCl engagement is unlikely to cause flaccid paralysis alone but may synergise with other targets; nAChR interactions, particularly for citronellol, could modulate cholinergic transmission, potentially interfering with worm motility; and Na^+/K^+-ATPase binding, though moderate, might add to ion homeostasis disturbance, especially if multiple monoterpenoids act simultaneously as present in the whole oil. We emphasise that all docking-derived predictions require experimental validation using target-specific assays, such as electrophysiology for ion channels, ATPase activity measurements, and bio-guided fractionation, to confirm which compound(s) drive the potent nematicidal effect observed *in vitro*. Nevertheless, the present *in silico* analysis provides a mechanistic hypothesis for the multi-target action of CNEO against *A. galli*.

We acknowledge that all four target structures originate from *C. elegans*. Although *C. elegans* and *A. galli* belong to the same nematode class (Chromadorea) and order (Rhabditia), and the residues lining each binding

cavity are well conserved within these protein families across nematode clades, the use of orthologue structures rather than *A. galli*-derived structures is an approximation; structure-resolved or homology-modelled *A. galli* counterparts would strengthen future studies. Furthermore, docking estimates binding affinity but does not measure functional modulation: a favourable predicted pose at AQP, GluCl, nAChR or Na^+/K^+-ATPase does not, by itself, demonstrate that water transport, chloride conductance, cholinergic neurotransmission or active ion exchange in the live worm is altered. Predicted multi-target engagement therefore generates a testable hypothesis rather than a confirmed mechanism.

Practically, our findings suggest that CNEO has potential as a complementary tool in poultry parasite control, particularly in low-input or organic free-range systems where chemical residues and resistance to synthetic anthelmintics are pressing concerns (Sajid *et al.*, 2022; Kapo *et al.*, 2025; Zoroaster *et al.*, 2025). CNEO may be further explored as a phytogenic feed supplement or supportive additive within integrated parasite-management programmes. Future work should prioritise (i) bio-guided fractionation of CNEO to confirm which constituents drive the observed mortality, (ii) head-to-head *in vivo* comparison with reference anthelmintics under matched assay conditions, (iii) functional assays at the four predicted targets (e.g. patch-clamp on heterologously expressed GluCl/nAChR, water-permeability assays for AQP, ATPase activity assays), (iv) *in vivo* efficacy, safety and pharmacokinetic studies in chickens, and (v) advanced delivery strategies such as nanoemulsion encapsulation to improve oil stability and bioavailability.

Conclusions: CNEO showed potent, concentration- and time-dependent *in vitro* nematicidal activity against adult *A. galli*, supported by histological and ultrastructural evidence of cuticular and reproductive damage. Predictive molecular docking of these three major components against four nematode targets generates a hypothesis of multi-target action that, if confirmed by functional assays, may help explain the observed activity.

Declarations

Funding: This research was funded by the Tropical Onehealth and EcoHealth Institute (TROPI) under grant number (grant no. 02/TROPI-GRANT/IV/2023), and by Universitas Sebelas Maret (UNS), Indonesia through its research support programme. Additional in-kind support was provided by the National Research and Innovation Agency (BRIN), Indonesia. The funders had no role in study design, data collection and analysis, decision to publish, or preparation of the manuscript.

Acknowledgement: The authors acknowledge the facilities, scientific and technical support form SEM and CryoEM Laboratory, National Research and Innovation Agency (BRIN).

We are also grateful to the Anatomical Pathology Laboratory, Faculty of Medicine, Universitas Gadjah Mada (UGM), for histological processing. We further acknowledge Rumah Atsiri, Karanganyar, Indonesia, for providing the *C. nardus* essential oil used in this study.

Conflict of interest: The authors declare that they have no conflicts of interest, financial or otherwise, that could have influenced the outcomes, interpretation or reporting of this research.

Data availability: All data generated or analysed during this study are included in this published article and its supplementary materials.

Ethical statement: Adult *A. galli* specimens were collected post-mortem from chickens during routine slaughterhouse processing at Ngebong Market, Boyolali Regency, Indonesia. No animals were handled, treated, anaesthetised or sacrificed for the purpose of this study. Field access and sample-collection activities were authorised by the National and Political Unity Agency (Kesbangpol, Central Java) under permit no. 070/642/XII/5.5/2021 (for a five-year research period). The study protocol was reviewed by the Animal Science Graduate Committee, Universitas Sebelas Maret (approval no. S-3B, 15 March 2023, granted to CWA), which formally waived the requirement for further ethical clearance because samples were obtained from carcasses generated by routine slaughter and no live animals were used. The study was conducted in accordance with applicable institutional and national guidelines.

Author's contribution: Chintianna Widhi Atthahirah (CWA) conducted the investigation, performed formal analysis and visualisation, and drafted the original manuscript. Penny Humaidah Hamid (PHH) developed the conceptual framework, supervised the study, performed funding acquisition and edited the manuscript. Herjuno Ari Nugroho (HAN) performed scanning electron microscopy, contributed to the investigation and edited the manuscript. Syahputra Wibowo (SW) performed molecular docking and contributed to formal analysis. Nur Balqis Maulydia (NBM) performed molecular docking. All authors read and approved the final version of the manuscript.

Generative AI statement: During the preparation of this work the authors used ChatGPT for sentence-level language polishing only. After using this tool the authors reviewed and edited the content as needed and take full responsibility for the content of the published article.

REFERENCES

Ali R, Rooman M, Mussarat S, *et al.*, 2021. A systematic review on comparative analysis, toxicology and pharmacology of medicinal plants against *Haemonchus contortus*. Frontiers in Pharmacology 12:750000.

Balqis U, Hambal M, Rinidar, *et al.*, 2017. Cuticular surface damage of *Ascaridia galli* adult worms treated with *Veitchia merrillii* betel nuts extract *in vitro*. Veterinary World 10:732-737.

Basyoni MM and Rizk EM, 2016. Nematodes ultrastructure: complex systems and processes. Journal of Parasitic Diseases 40:1130-1140.

Bennett J, Presswell B and Poulin R, 2023. Tracking life cycles of parasites across a broad taxonomic scale in a marine ecosystem. International Journal for Parasitology 53:285-303.

Berman HM, Battistuz T, Bhat TN, *et al.*, 2002. The Protein Data Bank. Acta Crystallographica Section D Biological Crystallography 58:899-907.

Carvalho VF, Ramos LDA, da Silva CA, *et al.*, 2020. *In vitro* anthelmintic activity of *Siparuna guianensis* extract and essential oil against *Strongyloides venezuelensis*. Journal of Helminthology 94:e50.

Decraemer W, Karanastasi E, Brown D *et al*., 2003. Review of the ultrastructure of the nematode body cuticle and its phylogenetic interpretation. Biological Reviews 78:465-510.

Espino Ureña MJ, Katchborian-Neto A, Trinidad AB, *et al*., 2023. Chemical composition, anthelmintic activity and mechanism of action of *Lippia dominguensis* Mold. essential oil on *Haemonchus contortus*. Chemistry & Biodiversity 20:e202300135.

Eberhardt J, Santos-Martins D, Tillack AF *et al*., 2021. AutoDock Vina 1.2.0: new docking methods, expanded force field and Python bindings. Journal of Chemical Information and Modeling 61:3891-3898.*et al*Frota AS, André WPP, Sales AB, *et al*., 2023. Anthelmintic activity of geraniol against gastrointestinal nematodes of small ruminants. Veterinary Parasitology 320:109996.

Hernando G, Turani O, Rodriguez Araujo N, *et al*., 2025. Unraveling anthelmintic targets and mechanisms of action of *trans*-cinnamaldehyde from cinnamon essential oil. Scientific Reports 15:5422.

Höglund J, Daş G, Tarbiat B, *et al*., 2023. *Ascaridia galli*-an old problem that requires new solutions. International Journal for Parasitology: Drugs and Drug Resistance 23:1-9.

Kapo N, Softić A, Goletić T, *et al*., 2025. Anthelmintic resistance in livestock farming: challenges and perceptions of farmers and veterinarians. Pathogens 14:1-15.

Kaur H, Bhardwaj U and Kaur R, 2021. *Cymbopogon nardus* essential oil: a comprehensive review on its chemistry and bioactivity. Journal of Essential Oil Research 33:205-220.

Krivak R and Hoksza D, 2018. P2Rank: machine learning based tool for rapid and accurate prediction of ligand binding sites from protein structure. Journal of Cheminformatics 10:39.

Lalthanpuii P and Lalchhandama K, 2020. Scanning electron microscopic study of the anthelmintic effects of some anthelmintic drugs on poultry nematode, *Ascaridia galli*. Advances in Animal and Veterinary Sciences 8:788-793.

Liu Y, Yang X, Gan J, *et al*., 2022. CB-Dock2: improved protein-ligand blind docking by integrating cavity detection, docking and homologous template fitting. Nucleic Acids Research 50:W159-W164.

Martinez-Ortiz-de-Montellano C, Torres-Acosta JFJ, Fourquaux I, *et al*., 2019. Ultrastructural study of adult *Haemonchus contortus* exposed to polyphenol-rich materials under *in vivo* conditions in goats. Parasite 26:65.

Matté EHC, Luciano FB and Evangelista AG, 2023. Essential oils and essential oil compounds in animal production as antimicrobials and anthelmintics: an updated review. Animal Health Research Reviews 24:1-11.

Nagaich S, 2022. Studies on the anthelmintic activity of *Syzygium aromaticum* oil on common poultry worms *Ascaridia galli* and *Heterakis gallinae*. Knowledgeable Research 1:68-73.

Nakahara K, Alzoreky NS, Yoshihashi T, *et al*., 2013. Chemical composition and antifungal activity of essential oil from *Cymbopogon nardus* (citronella grass). JARQ - Japan Agricultural Research Quarterly 47:249-252.

Nassar FS, 2025. Strategic role of poultry production sciences in shaping the future of global food security and strengthening sustainability. Poultry Science 104:106617.

Rasheed M and Aljohani ASM, 2024. Evaluation of anthelmintic effects of essential oil of star anise against *Ascaridia galli* of poultry. Pakistan Veterinary Journal 44:1223-1228.

Ristanti R, Iqbal M, Atthahirah CW, *et al*., 2023. Major intestinal parasites of domestic chicken in Boyolali, Central Java, Indonesia. Revista Electronica de Veterinaria 24:32-41.

Ristanti R, Hamid PH, Nugroho HA, *et al*., 2024. Anticoccidial activities of *Piper betle* L. essential oil on *Eimeria tenella* oocysts. Scientific Reports 14:25568.

Roy A, Khan A, Ahmad I, *et al*., 2022. Flavonoids - a bioactive compound from medicinal plants and its therapeutic applications. BioMed Research International 2022:5445291.

Sajid MS, Farhab M, Anjum FR, *et al*., 2022. Anthelmintic drug resistance in livestock: current understanding and future trends. In: Morales-Montor J, Del Río-Araiza VH and Hernandéz-Bello R (Eds.), Parasitic Helminths and Zoonoses - From Basic to Applied Research. IntechOpen: London.

Salem MOA, Alalwany RAS, Bassoss ASO *et al*., 2025. The impact of parasites on farm animal productivity: a review. Libyan Journal of Medical and Applied Sciences 3:115-120.

Saputra AA, Mulyadi D and Khumaisah LL, 2020. Uji efektivitas formula e-liquid minyak sereh wangi (*Cymbopogon nardus* L.) sebagai repelan terhadap *Aedes aegypti*. Chimica et Natura Acta 8:126-132.

Shohana NN, Rony SA, Ali MH, *et al*., 2023. *Ascaridia galli* infection in chicken: pathobiology and immunological orchestra. Immunity, Inflammation and Disease 11:e1001.

Situmorang PC, Wibowo S, Ilyas S, *et al*., 2025. *Rhodomyrtus tomentosa* attenuates HER2 expression and modulates apoptotic pathways in DMBA-induced breast carcinogenesis: *in vivo* and *in silico* insights. Journal of Agriculture and Food Research 19:102360.

Sukandar D, Sulaswatty A and Hamidi I, 2022. Profil senyawa kimia minyak atsiri sereh wangi (*Cymbopogon nardus* L.) hasil hidrodistilasi dengan optimasi perlakuan awal sonikasi. Alchemy Jurnal Penelitian Kimia 18:221-233.

Trindade LA, Cordeiro LV, de Figuerêdo Silva D, *et al*., 2022. The antifungal and antibiofilm activity of *Cymbopogon nardus* essential oil and citronellal on clinical strains of *Candida albicans*. Brazilian Journal of Microbiology 53:1231-1240.

Uopasai S, Senaphan K, Borlace GN, *et al*., 2024. *In vivo* mosquito repellency effect of citronella (*Cymbopogon nardus* (L.) Rendle) essential oil bath bomb formulation in dogs. Veterinary World 17:1538-1544.

Vijaya and Yadav CL, 2016. Standardisation of an *in vitro* adult worm motility assay for evaluating anthelmintic efficacy against *Ascaridia galli*. Journal of Parasitic Diseases 40:1389-1394.

Wei LS and Wee W, 2013. Chemical composition and antimicrobial activity of *Cymbopogon nardus* citronella essential oil against systemic bacteria of aquatic animals. Iranian Journal of Microbiology 5:147-152.

Wibowo S, Wardhani SK, Hidayati L, *et al*., 2024. Investigation of α-glucosidase and α-amylase inhibition for antidiabetic potential of agarwood (*Aquilaria malaccensis*) leaves extract. Biocatalysis and Agricultural Biotechnology 58:103152.

Zirintunda G, Biryomumaisho S, Kasozi KI, *et al*., 2021. Emerging anthelmintic resistance in poultry: can ethnopharmacological approaches offer a solution? Frontiers in Pharmacology 12:774896.

Zoroaster A, Singh Y, Simonato G, *et al*., 2025. Essential oils effectiveness against the most impactful parasites in poultry farming: a review. World's Poultry Science Journal 81:917-945.